HHS Public Access

Author manuscript

Cell Rep. Author manuscript; available in PMC 2023 January 09.

Published in final edited form as:

Cell Rep. 2022 November 22; 41(8): 111688. doi:10.1016/j.celrep.2022.111688.

Neutrophil inflammasomes sense the subcellular delivery route of translocated bacterial effectors and toxins

Changhoon Oh[1], **Lupeng Li**[2,3], **Ambika Verma**[1], **Arianna D. Reuven**[4], **Edward A. Miao**[2], **James B. Bliska**[4], **Youssef Aachoui**[1,5,*]

[1]Department of Microbiology and Immunology, University of Arkansas for Medical Sciences, Little Rock, AR 72205, USA

[2]Department of Immunology and Department of Molecular Genetics and Microbiology, Duke University, Durham, NC 27710, USA

[3]Department of Microbiology and Immunology, University of North Carolina at Chapel Hill, Chapel Hill, NC 27599, USA

[4]Department of Microbiology and Immunology, Geisel School of Medicine at Dartmouth, Hanover, NH 03768, USA

[5]Lead contact

SUMMARY

In neutrophils, caspase-11 cleaves gasdermin D (GSDMD), causing pyroptosis to clear cytosol-invasive bacteria. In contrast, caspase-1 also cleaves GSDMD but seems to not cause pyroptosis. Here, we show that this pyroptosis-resistant caspase-1 activation is specifically programmed by the site of translocation of the detected microbial virulence factors. We find that pyrin and NLRC4 agonists do not trigger pyroptosis in neutrophils when they access the cytosol from endosomal compartment. In contrast, when the same ligands penetrate through the plasma membrane, they cause pyroptosis. Consistently, pyrin detects extracellular *Yersinia pseudotuberculosis ΔyopM* in neutrophils, driving caspase-1-GSDMD pyroptosis. This pyroptotic response drives PAD4-dependent H3 citrullination and results in extrusion of neutrophil extracellular traps (NETs). Our data indicate that caspase-1, GSDMD, or PAD4 deficiency renders mice more susceptible to *Y. pseudotuberculosis ΔyopM* infection. Therefore, neutrophils induce pyroptosis in response to caspase-1-activating inflammasomes triggered by extracellular bacterial pathogens, but after they phagocytose pathogens, they are programmed to forego pyroptosis.

Graphical abstract

*Correspondence: yaachoui@uams.edu.

AUTHOR CONTRIBUTIONS

C.O., E.A.M., J.B.B., and Y.A. conceived the study. C.O., A.V., A.D.R., and L.L. performed the experiments and, together with E.A.M., J.B.B., and Y.A., analyzed the data. C.O. and Y.A. wrote the manuscript, and it was edited by C.O., E.A.M., J.B.B., and Y.A.

SUPPLEMENTAL INFORMATION

Supplemental information can be found online at https://doi.org/10.1016/j.celrep.2022.111688.

DECLARATION OF INTERESTS

The authors declare no competing interests.

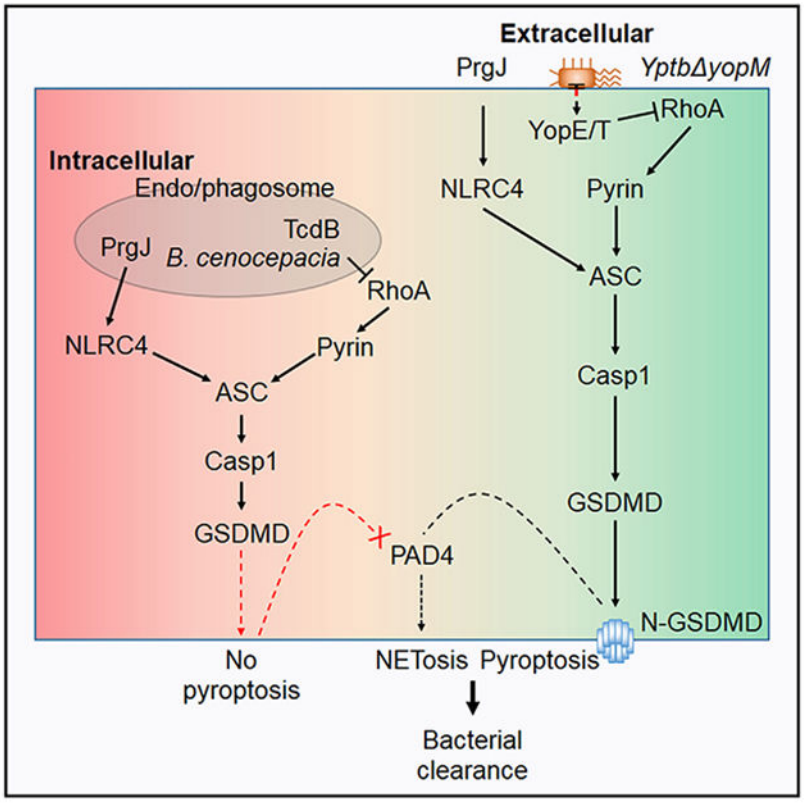

In brief

Oh et al. demonstrate that neutrophil caspase-1 inflammasomes selectively drive pyroptosis in response to bacterial virulence factors that are translocated across the plasma membrane. Consequently, neutrophil caspase-1-GSDMD-driven pyroptosis promotes PAD4-mediated histone citrullination and NET extrusion to protect against *Yptb-ΔyopM* infection.

INTRODUCTION

Pyroptosis is a lytic form of cell death that converts macrophages into pore-induced intracellular traps, driving inflammation and exposing pathogens to innate immune killing (Jorgensen et al., 2016). Inflammasomes are cytosolic sensors that detect microbial-associated molecular patterns or virulence factors, promoting pyroptosis and the release of interleukin (IL)-1β and IL-18 (Aachoui et al., 2013b). Once activated, the inflammasome recruits and activates either caspase-1 or −11. Active caspase-1 or −11 cleaves gasdermin D (GSDMD) to liberate its pore-forming N-terminal domain, promoting its trafficking to the cell membrane, pore formation, and subsequent plasma membrane rupture (Shi et al., 2015). Pyroptosis may also occur through parallel gasdermins when they are cleaved by other caspases or granzymes (Fischer et al., 2021).

Neutrophils regulate inflammasome sensing and the associated pyroptosis differently than macrophages. Unlike in macrophages, activation of caspase-1 inflammasome in neutrophils has generally been shown to drive IL-1β secretion without pyroptosis when activated by

NLRP3, AIM2, or NLRC4 (Chen et al., 2014; Karmakar et al., 2020; Kovacs et al., 2020; Son et al., 2021). In contrast, the parallel inflammatory caspase, caspase-11, does trigger GSDMD-driven pyroptosis in neutrophils, suggesting that neutrophils are not intrinsically resistant to GSDMD-driven pyroptosis (Chen et al., 2018; Kovacs et al., 2020).

Consequently, neutrophil caspase-11 activation and pyroptosis are critical to deny the bacteria a niche within neutrophils. Specifcally, we and Chen found that caspase-11 detects the cytosolic *Burkholderia thailandensis, Salmonella* Typhimurium *ΔsifA*, and *Shigella flexneri ΔospC3* lipopolysaccharide (LPS) presence and cleaves GSDMD to trigger neutrophil pyroptosis and NLRP3-processed IL-1β maturation (Chen et al., 2018; Kovacs et al., 2020; Oh et al., 2021). In addition, activated GSDMD drives neutrophil extracellular trap (NET) formation and extrusion (Chen et al., 2018), eliminating intracellular bacterial infections (Chen et al., 2018; Kovacs et al., 2020; Oh et al., 2021). In contrast, the inability of NLRC4 to cause pyroptosis, despite promoting a substantial amount of cleaved GSDMD, results in an overall defect in clearing the same infection. Indeed, we demonstrated that human-adapted *S. flexneri* employs T3SS OspC3 to prevent caspase-11-GSDMD-induced pyroptosis in neutrophils, enabling the bacteria to evade clearance despite detection by murine NLRC4 (Oh et al., 2021). It is strategically puzzling why neutrophils would inhibit this caspase-1 function *in toto* as it leaves the cytosol vulnerable. In addition, it has been shown that *Pseudomonas aeruginosa* infection leads to neutrophil pyroptosis in the absence of NOX2, albeit at low levels (Ryu et al., 2017). Therefore, we hypothesized that caspase-1, like caspase-11, could potentially promote pyroptosis in response to certain stimuli.

Pathogenic *Yersinia spp.*, including *Yersinia pseudotuberculosis (Yptb)* and *Yersinia pestis*, are primarily extracellular bacteria that use a contact-dependent T3SS to inject *Yersinia* outer proteins (Yops) into host cells to promote pathogenesis (Viboud and Bliska, 2005). These virulence effectors modulate multiple host signaling responses, which result in caspase-1 activation or inhibition. For instance, YopJ acetylates and inactivates TAK1, which is an important regulator of inflammatory cytokine products following Toll-like receptor (TLR) signaling (Paquette et al., 2012; Peterson et al., 2017). To counter TAK1 inhibition, naive macrophages activate caspase-8 to directly cleave GSDMD, which in turn promotes cell lysis and delayed caspase-1 activation (Monack et al., 1997; Philip et al., 2014). The same signaling pathway promotes caspase-3 activation to cleave GSDME in neutrophils (Chen et al., 2021). On the other hand, YopE and YopT inactivate the small GTPase RhoA to inhibit phagocytic signaling pathways (Viboud and Bliska, 2005). To counter this virulence, pyrin senses defective downstream signals of RhoA inactivation and signals to ASC for caspase-1 recruitment and activation, subsequently promoting cytokine release and macrophage pyroptosis (Xu et al., 2014). As disrupting the function of RhoA is critical for infection, *Yersinia spp.* use a second effector, YopM, to suppress pyrin activation (Chung et al., 2016; Ratner et al., 2016). Despite relatively high pyrin expression, the importance of the pyrin inflammasome in neutrophils remains unresolved. Since neutrophils are resistant to GSDMD-driven pyroptosis downstream of caspase-1, we questioned what utility the pyrin inflammasomes might provide during *Yersinia* infection. Furthermore, we hypothesize that neutrophils use a high level of pyrin expression to preserve pyroptosis inducibility, enabling other effector mechanisms even if RhoA is partly compromised.

Here, we examined neutrophil-specific caspase-1 inflammasome functionality by comparing the detection and clearance of extracellular *Yptb* and its *ΔyopM* mutant. We also combined the use of other inflammasome agonists and specific bacterial infections to investigate caspase-1 inflammasome outputs in neutrophils. Our results reveal that caspase-1 inflammasomes selectively drive pyroptosis in response to bacterial virulence factors that are translocated across the plasma membrane. In contrast, when neutrophils successfully phagocytose pathogens, they are programmed to forego pyroptosis in response to the virulence factors that are originated from bacteria-containing vacuoles.

RESULTS

Neutrophil detection of *Y. pseudotuberculosis* lacking YopM promotes two distinct signaling pathways to drive GSDMD- and GSDME-dependent pyroptosis

Neutrophils are among the primary innate immune cells recruited to the *Yersinia* infection site for bacterial clearance and are the major target of the T3SS-injected Yops (Marketon et al., 2005; Shannon et al., 2013). Chen et al. showed that neutrophils primed for a short time (3 h) respond to YopJ activity by programming caspase-8 to drive a rapid caspase-3-GSDME-mediated lysis (Chen et al., 2021). In contrast, when macrophages respond to YopJ manipulation, they program caspase-8 to directly cleave GSDMD, resulting in cell lysis and subsequent caspase-1 activation (Philip et al., 2014; Sarhan et al., 2018). However, it is still unclear if caspase-8 activation in neutrophils also promotes caspase-1 activation. To examine this, we primed wild-type (WT) or *Casp1*$^{-/-}$ bone-marrow-derived neutrophils (BMNs) for 3 h and infected them with *Yptb*-WT or its *ΔyopM* mutant. Regardless of caspase-1, *Yptb*-WT drove 10%–15% cytotoxicity in primed BMNs (Figure 1A). In contrast, infection with *Yptb-ΔyopM* results in a marked increase of caspase-1-dependent cytotoxicity (Figure 1A). To examine whether this cytotoxicity is dependent on either GSDMD or GSDME, we infected neutrophils deficient in GSDMD, GSDME, or both with *Yptb*-WT or *ΔyopM* mutant. Consistent with Chen et al.'s finding (Chen et al., 2021), *Yptb*-WT infection induces robust processing of full-length GSDME into the active p30 fragment and marginal GSDMD cleavage, resulting in GSDME-dependent lactate dehydrogenase (LDH) release (Figures 1B–1D). We also detect very weak IL-1β release, consistent with the lack of caspase-1 activation. Interestingly, *ΔyopM* mutant infection of WT BMNs results in strong cleavage of both GSDMD and GSMDE into their active p30 forms and promotes significant pyroptosis and IL-1β release (Figures 1B–1D). These inflammasome outputs are dependent on GSDMD for pyroptosis and either GSDMD or GSDME for IL-1β release (Figures 1B and 1C). More specifically, early in the infection (up to 2 h post infection), GSDMD is required for IL-1β release, but later on, GSDME can compensate for the loss of GSDMD to release IL-1β (Figures 1C and S1A). GSDMD-deficient neutrophils exhibit sublytic activation of GSDME likely through bypass pathways at caspase-1-BID branching, allowing delayed IL-1β release. Together, our data suggest that caspase-1 activation by the *ΔyopM* mutant promotes GSDMD-induced pyroptosis in neutrophils. This supports our hypothesis that there are certain situations where caspase-1 can cause pyroptosis in neutrophils.

To examine whether YopJ plays a role in caspase-1-mediated pyroptosis, we infected primed WT BMNs with *Yptb*-WT or the *yopJ*^{C172A} mutant, which lacks acetyltransferase

activity. We also compared these with strains on a *ΔyopM* background. In response to YopJ catalytic activity, neutrophils trigger the cleavage of GSDME into its pore-forming p30 form, promoting the associated cytotoxicity (Figures 1E–1G, S1B, and S1C). As expected, in the absence of YopM, *Yptb* infection leads to caspase-1 activation. However, in a *yopM* and *yopJ* double mutant, both pyroptosis and IL-1β release were enhanced (Figures 1E–1G). This indicates that the activity seen in a single *yopM* mutant is actually being partially inhibited by YopJ catalytic activity. These data support the previous report that both YopM and YopJ can independently inhibit caspase-1 (Schoberle et al., 2016) and extend that finding from macrophages to neutrophils.

Pyrin drives neutrophil caspase-1-dependent pyroptosis in response to *Y. pseudotuberculosis* Δ*yopM* infection

Since our results in Figure 1 indicate that neutrophils undergo caspase-1 pyroptosis in response to infection with *Yptb* lacking YopM, we examined whether pyrin drives neutrophil pyroptosis through caspase-1. To do this, we primed WT, *Casp1*$^{-/-}$, and *Mefv*$^{-/-}$ BMNs (and bone-marrow-derived macrophages [BMMs] for comparison) for 16 h with a low dose of LPS and interferon (IFN)-*γ*. We found that under this priming regimen, neutrophils spontaneously display weak bands of cleaved apoptotic caspase-3 and -7 and marginal GSDME p30 (Figure S2A). Accordingly, over 80% of the cells are annexin V-propidium iodide (PI) double negative and have not released LDH (Figures S2B and S2C), suggesting that these cells have not undergone apoptosis or lytic cell death. These data are consistent with recent reports reviewed in Miralda et al., (2017), indicating that priming prolongs neutrophil lifespan by activating anti-apoptotic signaling pathways and downregulating pro-apoptotic gene expression. Of relevance to this study, under this priming condition, macrophages limit their response to YopJ while simultaneously priming multiple inflammasome pathways (Bergsbaken and Cookson, 2007). As expected, in response to *Yptb*-WT infection, longer priming reduced caspase-8 activation and subsequent GSDME cleavage, both in BMMs and BMNs, resulting in significantly reduced LDH release (Figures 2A–2F). Interestingly, BMNs also respond in a similar fashion as BMMs to *Yptb-ΔyopM* infection. Both cells display comparably robust caspase-1 and GSDMD cleavages, promoting pyroptosis and IL-1β secretion (Figures 2A–2F and S2D). These phenotypes are recapitulated in short-primed BMNs with *Yptb-yopJ*^{C172A}*ΔyopM* mutant infection (Figures S2E–S2G). Additionally, both BMNs and BMMs dephosphorylate pyrin at S205, indicative of its activation, upon *Yptb-ΔyopM* infection (Figures 2C and 2F). Consistently, BMNs fail to activate caspase-1-dependent pyroptosis and IL-1β secretion in the absence of pyrin (Figures 2G–2I). These results indicate that neutrophils are not intrinsically resistant to caspase-1 pyroptosis following pyrin inflammasome activation.

Neutrophil pyrin inflammasome discriminates between agonists that access the cytosol from the plasma membrane or vacuolar route to promote pyroptosis

It was surprising that neutrophil pyrin activation of caspase-1 triggers pyroptosis since, in response to similar activation of caspase-1 via either NLRC4, NLRP3, or AIM2, neutrophils do not undergo pyroptosis (Chen et al., 2018; Karmakar et al., 2020; Kovacs et al., 2020; Son et al., 2021). Therefore, we investigated the mechanisms that regulate this dichotomous response. First, we examined whether pyrin generally triggers neutrophil

pyroptosis. TcdB is a major virulence factor of *Clostridium difficile*, which also inactivates RhoA by glycosylation, triggering pyrin activation (Just et al., 1995; Xu et al., 2014). TcdB is translocated into the cell through receptor-mediated endocytosis and requires endosomal acidification for the complete release of glucosyltransferase domains into the cytosol (Barth et al., 2001; Qa'Dan et al., 2000). To simplify the study of this toxin, LFn fused to enzymatically active TcdB is often used to probe its function (Spyres et al., 2001). To investigate whether TcdB triggers pyrin-dependent pyroptosis in neutrophils, we stimulated 16 h primed BMMs and BMNs with LFn-TcdB treatment. In response to LFn-TcdB, primed BMMs undergo caspase-1-dependent pyroptosis and mature IL-1β release (Figures 3A, 3B, and 3E). In response to the same agonist, BMNs dephosphorylate pyrin at S205 and cleave caspase-1 and GSDMD to their mature forms like BMMs but, surprisingly, release mature IL-1β without pyroptosis (Figures 3C, 3D, and 3F). This response contrasts with *Yptb-ΔyopM* infection, where both mature IL-1β release and pyroptosis are triggered in a pyrin- and caspase-1-dependent manner in neutrophils (Figures 3C, 3D, and 3F).

Burkholderia cenocepacia is a vacuolar bacterium that uses the T6SS effector TecA to deamidate RhoA, which is detected by pyrin (Aubert et al., 2016), providing us with a third agonist to activate pyrin. While 16 h primed WT BMMs activated caspase-1 and pyroptosis and released mature IL-1β in response to *B. cenocepacia* infection, primed WT neutrophils did not trigger pyroptosis, despite the activation of both caspase-1 and GSDMD by pyrin (Figures 3G–3L, S3A, and S3B). Because failure to trigger pyroptosis also occurred with purified LFn-TcdB, these data suggest that neutrophils employ an unknown regulatory mechanism to limit pyrin-induced pyroptosis. This led us to question how pyrin discriminates between three inhibitors of RhoA in neutrophils but not in macrophages. Intriguingly, *Yptb-ΔyopM* uses a T3SS to inject YopE/T through a plasma membrane, whereas LFn-TcdB and *B. cenocepacia* TecA enter the cytosol across endosomal membranes.

Therefore, we hypothesized that the site of membrane translocation of these RhoA-inactivating agonists determines whether neutrophils undergo pyroptosis in response to caspase-1 activation. To examine this hypothesis, we compared activation of the pyrin inflammasome in neutrophils via translocation of LFn-TcdB through the endocytic pathway versus by direct electroporation across the plasma membrane. The LFn-TcdB in this study is constructed by using the enzymatically active portion of TcdB ($TcdB_{1–556}$) and thus does not require endosome acidification for activation of the toxin enzyme (Spyres et al., 2001). Translocation of LFn-TcdB to the cytosol using either PA or electroporation resulted in caspase-1-dependent IL-1β maturation (Figure 3M). However, only electroporation of this TcdB into the cytosol triggered caspase-1-dependent pyroptosis of neutrophils (Figure 3N). Because we have previously reported that only caspase-11 triggers GSDMD-mediated pyroptosis in neutrophils (Kovacs et al., 2020), we performed the same treatments using caspase-11-deficient BMNs to exclude the effect of putative LPS contamination in purified bacterial toxins. As expected, the absence of caspase-11 affected neither caspase-1-dependent pyroptosis nor IL-1β secretion in treated neutrophils (Figures S3C and S3D). This result suggests that neutrophil pyrin does not promote pyroptosis based on the type of the RhoA inactivation but rather based on the location of translocation into the cytosol.

Neutrophil NLRC4 inflammasomes detect membrane-dependent T3SS injection and respond by driving caspase-1 pyroptosis

Compared with macrophages, neutrophils express much less NLRC4, somewhat less caspase-1, and slightly less ASC. Conversely, neutrophils express far more pyrin, though pyrin in both cell types is inducible by TLR agonists and type II IFNs (Figure S4A). We previously hypothesized that low expression caused NLRC4 to poorly activate caspase-1, resulting in insufficient GSDMD cleavage, and thereby pyroptosis did not occur (Aachoui et al., 2015; Miao et al., 2010). However, we found that infection with vacuolar bacteria *S. typhimurium* or cytosolic bacteria *B. thailandensis* and *S. flexneri* promotes robust cleavages of caspase-1 and GSDMD, as well as IL-1β release, but no concomitant cell death in BMNs, unlike BMMs (Figures 4A–4C and S4B–S4D).

Therefore, we asked whether the NLRC4 inflammasome, similarto pyrin, could also differentially respond to plasma-membrane-penetrating effectors as opposed to endocytically delivered effectors. To examine this, we compared neutrophil responses to the detection of LFn-PrgJ when translocated to the cytosol by PA with delivery by electroporation. Remarkably, electroporation of LFn-PrgJ caused neutrophils to undergo caspase-1-dependent pyroptosis independently of caspase-11 (Figures S3C and S3D), whereas PA delivery did not cause pyroptosis (Figures 4D, 4E, S4E, and S4F). This correlated with significant IL-1β release following endocytic delivery with PA. Next, we verified that our electroporation and LFn/PA delivery system promoted the translocation of bacterial effectors to the cytosol through distinct routes. Specifically, we stimulated BMNs with LFn-PrgJ by either method in the presence or absence of cytochalasin D, an actin polymerization inhibitor that prevents phagocytosis/endocytosis (Figure S4G). Cytochalasin D treatment significantly suppresses IL-1β release and GSDMD cleavage following stimulation through the LFn/PA system but not by electroporation. Thus, our results confirm that electroporation and the LFn/PA system use plasma-membrane-penetrating and endocytic routes, respectively, to deliver bacterial effectors. To further investigate the ability of neutrophil NLRC4 to distinguish T3SS activity that originated at the plasma membrane from the endosome, we examined the caspase-1 response to extracellular T3SS-expressing bacteria, comparing *P. aeruginosa* strains PAO1 and PAK with *S. typhimurium*, in neutrophils and macrophages. In line with our previous observation, BMNs infected with *S. typhimurium* selectively trigger GSDMD cleavage and IL-1β processing without concomitant pyroptosis (Figures 4A–4C and 4F–4H). This is in contrast to BMMs, where *S. typhimurium* detection promotes IL-1β release and pyroptosis (Figures S4B–S4D, S4H, and S4I). In support of our hypothesis that neutrophils induce pyroptosis in response to caspase-1-activating inflammasomes triggered by extracellular bacterial pathogens, infection by either PAO1 or PAK triggers caspase-1-dependent GSDMD cleavage and IL-1β and LDH release in both cells (Figures 4F–4H, S4J, and S4K). A similar phenotype was observed following neutrophil infection with PAO1 mutant lacking ExoS, an exoenzyme that inhibits ROS production (Vareechon et al., 2017) (Figures S4J and S4K), suggesting that this function is not responsible for caspase-1-driven pyroptosis in neutrophils.

Altogether, these results demonstrate that the caspase-1-activating inflammasomes discriminate stimuli originating from the vacuole versus the plasma membrane, at least when NLRC4 or pyrin are triggered.

Caspase-1 pyroptosis promotes PAD4-dependent histone citrullination and NET formation

Recent studies indicate that GSDMD activation can cause NETosis. For instance, it has been reported that NE-cleaved GSDMD drives chromatin expansion and NETosis in phorbol myristate acetate (PMA)-activated neutrophils (Sollberger et al., 2018). However, unexpectedly, in a separate study, NLRC4 inflammasome activated GSDMD but promoted neither chromatin decondensation nor NETosis (Chen et al., 2018). Chromatin relaxation can also be mediated through protein arginine deiminase 4 (PAD4), which drives NETosis (Wang et al., 2009). PAD4 is a deiminase capable of converting arginine (positive charge) into citrulline (neutral), inactivating histone 3, and subsequently relaxing DNA. PAD4 requires elevated calcium concentrations for activation of its enzymatic function to citrullinate histones (Arita et al., 2004; Kearney et al., 2005). However, the complete mechanism of PAD4 activation and the reason why caspase-1 is not conducive to chromatin expansion in neutrophils despite promoting GSDMD cleavage by NE are unclear. Therefore, we asked whether pyroptosis inducibility by neutrophil caspase-1 is responsible for chromatin decondensation. To test this hypothesis, we used immunoblotting to probe for H3 citrullination following infection of primed (16 h) WT, *Casp1*$^{-/-}$, *Gsdmd*$^{-/-}$, or *Gsdme*$^{-/-}$ neutrophils with *Yptb*-WT or *ΔyopM*. Our results show that caspase-1 activation following pyrin detection of *Yptb-ΔyopM* promotes H3 citrullination that is dependent on cleavage of GSDMD to its p30 form and the associated lysis (Figures 5A and 5B). Under short-priming conditions, neutrophils respond to YopJ by promoting the p30 form of GSDME, driving cell lysis without NETs (Chen et al., 2021). Consistently, infections of short-primed WT, *Gsdmd*$^{-/-}$, or *Gsdme*$^{-/-}$ neutrophils with *Yptb*-WT, *yopJ*^{C172A}, or *yopJ*^{C172A} *ΔyopM* mutants indicate that GSDME-mediated cell lysis is dispensable for histone H3 citrullination, unlike GSDMD-driven pyroptosis (Figure S5A). Treatment with the NE inhibitor sivelestat, which inhibits NET formation in some cases, did not impede histone H3 citrullination by *Yptb-ΔyopM* (Figure 5C) or *yopJ*^{C172A} *ΔyopM* mutants (Figure S5B). Therefore, NE is dispensable for this function. As expected, despite undergoing pyroptosis, PAD4-deficient neutrophils infected with *Yptb-ΔyopM* did not display histone H3 citrullination (Figures 5D and 5E). In addition, *P. aeruginosa* triggered H3 citrullination along with neutrophil pyroptosis, whereas *B. cenocepacia* did not (Figures 5D and 5E).

Next, we examined how GSDMD-driven pyroptosis and PAD4-dependent H3 citrullination are connected. Since PAD4 is a Ca^{2+}-dependent enzyme, we examined if Ca^{2+} influx through GSDMD pores drives PAD4 activation. Our results show that *Yptb-ΔyopM* infection in Ca^{2+}-free media does not result in H3 citrullination, despite triggering neutrophil pyroptosis as in Ca^{2+}-supplemented media (Figure S5C). These results imply that GSDMD pore-mediated Ca^{2+} influx promotes PAD4-driven NET formation during *Yptb-ΔyopM* infection.

Next, we investigated whether caspase-1-driven pyroptosis and the associated PAD4-dependant H3 citrullination is conducive to NET extrusion. To examine this hypothesis,

we monitored for extracellular DNA presence, indicative of NET extrusion, with the cell-impermeable DNA-binding dye Sytox green after infection of WT, *Casp1*$^{-/-}$, or *Gsdmd*$^{-/-}$ neutrophils with *Yptb*-WT or *ΔyopM* (Figures 5F, S5D, and S5E). Consistent with the dependence of histone H3 citrullination on caspase-1 and GSDMD, the release of NETs by *Yptb-ΔyopM* infection was also dependent on caspase-1 and GSDMD. Additionally, these NET structures were sensitive to DNase I treatment *in vitro*, supporting the hypothesis that caspase-1-triggered pyroptosis in neutrophils drives NET extrusion. Interestingly, PAD4 deficiency in neutrophils was dispensable to caspase-1 pyroptosis but essential to histone H3 citrullination and the subsequent NET formation in response to *Yptb-ΔyopM* (Figures 5D, 5E, 5G, and 5H). To determine whether caspase-1-GSDMD pyroptosis-driven NETs promote bacterial clearance, we infected WT, *Casp1*$^{-/-}$, or *Gsdmd*$^{-/-}$ neutrophils with *Yptb*-WT or *ΔyopM* in the presence of DNase I or not. Consistent with the absence of NETs, *Yptb*-WT comparably survives in all three neutrophil types tested regardless of DNase I treatments (Figure S5F). In contrast, *Yptb-ΔyopM* survival was restricted in WT neutrophils compared with *Casp1*$^{-/-}$ and *Gsdmd*$^{-/-}$ neutrophils (Figure S5G). Additionally, DNase I treatment restored the survival of *Yptb-ΔyopM* in WT neutrophils (Figure S5G), suggesting that caspase-1-GSDMD pyroptosis-driven NETs are critical for neutrophil anti-microbial activity *in vitro*.

These results indicate that PAD4 is activated in response to caspase-1-GSDMD-induced pyroptosis and mediates histone H3 citrullination and NETs. However, PAD4 is dispensable for caspase-1-mediated pyroptosis following extracellular bacterial infection tested here.

Neutrophil pyrin-dependent GSDMD and PAD4 activations are critical in defense against *Y. pseudotuberculosis* Δ*yopM*, whereas GSDME is deleterious

Next, we examined whether GSDMD or GSDME deficiency renders mice more susceptible to *Yptb-ΔyopM* infection. Even though previous studies have demonstrated that caspase-1 and pyrin are important for the defense against systemic *Yptb-ΔyopM* infection *in vivo* (Chung et al., 2016; LaRock and Cookson, 2012), the competing roles of GSDMD and GSDME during this infection remains unsolved. First, we confirmed the phenotypes of *Yptb-ΔyopM* infection in WT, *Casp1*$^{-/-}$, and *Mefv*$^{-/-}$ mice. As expected, *Casp1*$^{-/-}$ and *Mefv*$^{-/-}$ mice were extremely susceptible to *Yptb-ΔyopM* and succumbed within 9 days post-infection (Figures S6A and S6B). Next, we examined the susceptibility of WT, *Gsdmd*$^{-/-}$, and *Gsdme*$^{-/-}$ mice to *Yptb-ΔyopM* infection. We found that the attenuation of the *Yptb-ΔyopM* mutant is reversed in *Gsdmd*$^{-/-}$ mice with similar kinetics as *Casp1*$^{-/-}$, indicating that GSDMD activation by caspase-1 is essential in host defense against *Yptb-ΔyopM* (Figures 6A–6C and S6B–S6D). In response to *Yptb-ΔyopM*, *Gsdmd*$^{-/-}$ mice harbor between 10 and 100 times higher bacterial burdens in the spleen and liver, respectively, than WT and *Gsdme*$^{-/-}$ mice at day 5, which subsequently result in extreme susceptibility and morbidity at days 6–8 (Figures 6A–6C). In contrast, 80% of WT and 100% of *Gsdme*$^{-/-}$ mice resist the infection through day 21, when the experiment was terminated (Figure 6A). To examine whether lack of cytokine secretion cause the susceptibility in *Gsdmd*$^{-/-}$ mice, we infected WT, *Il1b*$^{-/-}$, *Il18*$^{-/-}$, or *Il1b-Il18*^{DKO} mice with *Yptb-ΔyopM*. Even though *Il1b-Il18*^{DKO} mice display about 20 times higher bacterial burdens in liver, cytokine-defective mice were significantly less susceptible to *Yptb-ΔyopM*

compared with *Gsdmd*$^{-/-}$ mice (Figures S6E and S6F). This suggest that GSDMD-mediated inflammasome activation plays other important roles for anti-bacterial immune response (Figures S6E and S6F).

When the yopM expressing *Yptb*-WT is examined, all these GSDMD-mediated defenses were lost. Infection of WT, *Gsdmd*$^{-/-}$, and *Gsdme*$^{-/-}$ mice resulted in similar bacterial burdens in liver and spleen at day 5, which correlated with in WT and *Gsdmd*$^{-/-}$ mice succumbing to infection at day 7 (Figures 6D–6F). On the other hand, the trending difference of *Gsdme*$^{-/-}$ mice to be more resistant to infection seen with the *ΔyopM* mutant was recapitulated and reached statistical significance with *Yptb*-WT, where *Gsdme*$^{-/-}$ mice survived for 2–3 days longer but, nevertheless, succumbed to infection as well at day 10 (Figure 6D). This result indicates that in the presence of YopM, detection of *Yersinia* and activation of GSDME downstream of YopJ actually plays a deleterious role for host defense.

Since the GSDMD-driven pyroptosis in neutrophils is associated with PAD4-dependant H3 citrullination and NET formation, but GSDME-mediated cell lysis is not, we examine the importance of PAD4 in murine immune defense against *Yptb-ΔyopM*. We infected *Padi4*$^{-/-}$ mice as above and examined survival and bacterial burdens in the spleen and liver. Even though WT and *Padi4*$^{-/-}$ mice displayed comparable bacterial burden in liver and spleen at day 5 (Figures S6G and S6H), about 70% of mice succumbed to infection at days 7–12 with slower kinetics than *Casp1*$^{-/-}$ mice, while WT mice survived, indicating that PAD4 is important for defense against *Yptb-ΔyopM* infection (Figure 6G). Other mechanisms, such as cytokine secretion and the release of cytosolic bactericidal molecules by pyroptosis, likely compensate partially for PAD4 deficiency to fight the infection. To examine whether NETs are one of the important mechanisms of bacterial clearance driven by GSDMD and PAD4, we dismantled NETs *in vivo* by daily application of DNase I after *Yptb-ΔyopM* infection, as has been used by other investigators to investigate NETs *in vivo* (Agarwal et al., 2019; Chen et al., 2018). DNase I treatment resulted in a significantly increased bacterial burden in the WT spleen and liver, but not in *Casp1*$^{-/-}$, at day 4 (Figures 6H and 6I), suggesting that caspase-1-dependent NETs are critical to clear the *Yptb-ΔyopM* mutant.

DISCUSSION

One interesting feature of neutrophils is their remarkable resistance to caspase-1-induced pyroptosis relative to macrophages. Surprisingly, we have now found that caspase-1-induced pyroptosis is not suppressed in neutrophils but instead is highly regulated. Our data show that caspase-1 pyroptosis occurs when virulence factor agonists cross the plasma membrane. If the same agonists cross endosomal membranes, neutrophils activate caspase-1 but resist lysis. We speculate that these two distinct caspase-1 phenotypes are likely the result of structural peculiarities of neutrophils. Since the neutrophil cytosol is dense, packed with primary, secondary, and tertiary granules, inflammasome activation of caspase-1 in close proximity to endosome likely meets a physical hindrance, obstructing N-GSDMD from reaching the cell membrane (Karmakar et al., 2020). In contrast, GSDMD activation in close proximity to plasma membrane, but away from granules, is conducive to its insertion into the plasma membrane and subsequent pyroptotic lysis of the neutrophils.

Strategically, this intrinsic regulation of pyroptosis inducibility orchestrates neutrophil defense following sensing of the bacterium. If a neutrophil detects a bacterium that injects virulence factors from within the neutrophil phagosome, dispatching IL-1β to alert innate and adaptive immune cells without pyroptosis could be sufficient to contain the infection. Indeed, Miao et al. showed that *S. typhimurium* accumulate in neutrophils following efferocytosis of bacteria entrapped within pore-induced intracellular traps (PITs) (Jorgensen et al., 2016; Miao et al., 2010). Thereafter, they are eliminated in neutrophils in a NADPH-oxidase-dependent fashion without the need to pyroptose. On the other hand, extracellular bacteria that suppress efficient phagocytosis evade phagocytic killing. Countering these bacteria, neutrophils deploy another anti-microbial strategy, NETs. NETs are extracellular web-like structures made up of decondensed chromatin and various anti-microbial peptides. They efficiently trap and neutralize a broad range of microbes. If neutrophils detect virulence factors, which hijack the cell metabolism, from extracellular bacteria such as *Yersinia* and *Pseudomonas*, this leads to the cleavage GSDMD in a caspase-1-dependent manner to trigger pyroptosis. As it appears that the process of pyroptosis does not directly kill the bacteria in macrophages, neutrophils wired caspase-1-GSDMD-mediated pyroptosis to drive histone citrullination by activating PAD4. We show here that chromatin expansion consequently releases NETs during *Yptb-ΔyopM* infection. Furthermore, our *in vitro* and *in vivo* results, using DNase I application to dismantle extruded NETs, and the higher susceptibility of PAD4-deficient mice to *Yptb-ΔyopM* suggest that PAD4-dependent NETs are an important factor to clear bacterial infection by caspase-1 inflammasome.

The mechanism of coupling pyroptosis and NETs, whether through caspase-1 or -11 inflammasomes, could enables neutrophils to counter both extracellular T3SS-mediated injection of virulence effectors and cytosolic presence of LPS. Under such pressure, Gram-negative bacteria evolved a mechanism to subvert this neutrophil defense, either by sequestering inside a vacuole or directly inhibiting inflammasome sensing (Aachoui et al., 2013a; Brodsky et al., 2010; Chung and Bliska, 2016; Cunha and Zamboni, 2013; LaRock and Cookson, 2012; Sutterwala et al., 2007). Interestingly, our data reveal that bacteria can also deploy a more offensive strategy to subvert and exploit neutrophil pyroptosis. By comparing neutrophil response to *Yptb* in the presence or absence of gasdermins, we and Chen et al. found that the *Yptb*-WT can trigger a parallel pyroptotic inflammasome, caspase-8-GSDME, that kills neutrophils without the associated NETs and little release of IL-1β (Chen et al., 2021). In a *Yersinia* systemic infection model, unlike the oral infection model, deletion of GSDME extended the survival of infected animals for a few days, suggesting that this pyroptosis mechanism is deleterious for host defense. Although we cannot exclude the contribution of other cell types, we speculate that this NET-free pyroptosis is not compatible to clear extracellular bacteria and might reduce the pool of neutrophils and subsequent cytokine production or total bactericidal capabilities of neutrophils.

PAD4 has emerged as an important driver of NETosis by inactivating histones to relax chromatin. Furthermore, PAD4 was shown to be critical for the whole process of NETosis including chromatin decondensation, nuclear envelope rupture, and extracellular DNA expulsion during ionomycin-mediated NETs (Thiam et al., 2020). However, we found that PAD4 activation was dispensable for caspase-1-driven pyroptosis yet was critical in defense

against *Yptb-ΔyopM*. The importance of PAD4 is diminished in other circumstances; for instance, during caspase-11-dependent NETs, PAD4 is dispensable for both caspase-11-GSDMD-driven pyroptosis and defense against cytosol-invasive pathogens, even though it is responsible for histone H3 citrullination (Chen et al., 2018). Unlike caspase-1, caspase-11 compensates for the role of histone citrullination by degrading histones to decondense chromatin. NE, as well, is known to drive histone degradation and chromatin decondensation (Papayannopoulos et al., 2010). Endocytic stimuli-mediated caspase-1 activation does not drive PAD4 activation but instead drives NE release from neutrophil granules (Karmakar et al., 2020). However, this does not trigger histone degradation nor PAD4 activation. These observations suggest that GSDMD pores in other membrane are likely needed at two levels that cannot be met in the absence of a conducive pyroptosis stimulation: first, likely at the nuclear membrane to enable NE access to chromatin, and second, at a major calcium source, such as the endoplasmic reticulum (ER) or plasma membrane. Because we did not directly assess the anti-bacterial role of NE in the context of our infections that promote GSDMD pyrpotosis, we cannot exclude a role of NE downstream of histone citrullination. However, it appears that NE is insufficient to compensate for PAD4 function in chromatin relaxation since PAD4-deficient mice succumbed to infection with *Yptb-ΔyopM*. Therefore, the exact mechanism of PAD activation and steps leading to chromatin expansion will be the subject of future studies. In summary, our study demonstrates caspase-1 as a master regulator of neutrophil defenses against extracellular T3SS Gram-negative bacteria.

Limitations of the study

In this study, we found that neutrophils display distinct responses to bacterial effectors depending on the subcellular delivery route. However, the mechanism by which plasma-membrane-penetrating, but not endocytic, inflammasome stimuli induce neutrophil pyroptosis has not been addressed in this study. We also observed that *Yptb-ΔyopM*, but not *Yptb*-WT, infection leads to pyroptosis-mediated PAD4 activation and subsequent NET formation, even though both bacterial strains can induce pyroptosis via different signaling pathways. Because both types of pyroptosis can allow extracellular Ca^{2+} influx, future studies need to address this discrepancy between the consequence of GSDMD and GSDME pyroptosis.

STAR★METHODS

RESOURCE AVAILABILITY

Lead contact—Further information and requests for resources and reagents should be directed to and will be fulfilled by the lead contact, Youssef Aachoui (YAachoui@uams.edu).

Materials availability—All materials are available from the corresponding author upon reasonable request.

Data and code availability—All data reported in this paper will be shared by the lead contact upon request.

This paper does not report original code.

Any additional information required to reanalyze the data reported in this paper is available from the lead contact upon request.

EXPERIMENTAL MODEL AND SUBJECT DETAILS

Bacterial strains— *Y. pseudotuberculosis* (32777) wild-type, *yopM, yopJ*^{C172A} *and yopJ*^{C172A}*ΔyopM* mutants (McPhee et al., 2010; Schoberle et al., 2016; Simonet and Falkow, 1992), *S.* Typhimurium (CS401)(by Samuel I Miller), *P. aeruginosa* (PAO1 and PAK)(by Colin Manoil and Bob Ernst), and *B. cenocepacia* (Maltez et al., 2015).

Y. pseudotuberculosis strains were grown in Luria-Bertani (LB) broth at 28°C. *S.* Typhimurium, *P. aeruginosa*, and *B. cenocepacia* were grown in LB broth at 37°C. *Y. pseudotuberculosis* strains were grown overnight and further diluted (1:40) in LB broth containing 20 mM sodium oxalate and 20 mM $MgCl_2$, and grown at 28°C for 1 hr, then shifted 37°C for 2 hr for the use of *in vitro* experiments (Schoberle et al., 2016). Other bacteria strains were grown overnight and further diluted (1:40) in LB broth and grown at 37°C for 3 hr.

Mice—Wild type C57BL/6 (Jackson # 000664), *Casp1*$^{-/-}$ (Jackson # 032662), *Casp1*$^{-/-}$ (Kayagaki et al., 2011), *Casp1-Casp11*^{DKO} (Kuida et al., 1995), *Nlrc4-Asc*^{DKO} (Aachoui et al., 2015), *Gsdmd*$^{-/-}$ (Jackson # 032663), *Gsdme*$^{-/-}$ (Jackson # 032411), *Mefv*$^{-/-}$ (Chae et al., 2011), and *Padi4*$^{-/-}$ (Jackson # 030315) mice were used in this study. We crossed *Gsdmd*$^{-/-}$ with *Gsdme*$^{-/-}$ to generate *Gsdmd-Gsdme*^{DKO}. All mice used in this study were in C57BL/6 genetic background and were bred and housed up to five mice per ventilated cage in a specific pathogen-free facility at the University of Arkansas for Medical Sciences. Both female and male mice aged between 6 and 10 weeks were used for all animal experiments. All protocols met the guidelines of the US National Institutes of Health for the humane care of animals and were approved by the Institutional Animal Care and Use Committee at the University of Arkansas for Medical Sciences.

Bone marrow-derived macrophages (BMMs)—Bone marrow was extracted from tibias and femurs of both male and female mice. Progenitor cells were cultured in Dulbecco's Modified Eagle's Medium (DMEM) supplemented with 10% fetal bovine serum (FBS), 2 mM L-glutamine, 1% penicillin/streptomycin and 20% L929 cell-conditioned media. Fresh medium was added at day 4 and differentiated BMMs were harvested at day 7. All cells were incubated at 37°C, 5% CO2.

METHOD DETAILS

Bone marrow-derived neutrophils (BMNs) isolation—BMNs were isolated from murine bone marrow using a Neutrophil Isolation Kit (Miltenyi Biotec) according to the manufacturer's instructions.

***In vivo* infection—**Single colony of wild type *Y. pseudotuberculosis* and *ΔyopM* mutant were grown overnight at 28°C. Bacteria were centrifuged, washed three times with phosphate-buffered saline (PBS), and prepared as 1 mL PBS suspensions containing 1 ×

10^4 colony forming units (CFU). 2×10^3 CFU of bacteria were infected through tail vein (i.v.) injection. At 5 d post-infection, spleens and livers were collected and homogenized in sterile PBS. Viable CFU were enumerated by plating serial dilutions on LB agar plates. For lethal challenges, mice were monitored at least twice daily for 21 d.

***In vitro* infection and stimulation—**For *in vitro* infection, BMMs and BMNs were seeded into 96-well plates at a density of 1×10^5 cells/well and 5×10^5 cells/well respectively. Cells were primed for 3 hr with 100 ng/mLof LPS and IFN-γ or for 16 hr with 50 ng/mL of LPS and IFN-γ, followed by infection with bacteria at a multiplicity of infection (MOI) of 30 in opti-MEM. Cells were immediately centrifuged at 700 x g for 10 min at room temperature, and then incubated at 37°C for 1 hr before adding 100 μg/mL of gentamicin to eliminate extracellular bacteria. Supernatants or cell lysates were collected at indicated time points. For bacterial CFU assay, infected BMNs were added with DNase I (Promega, 20 U/mL) or not without gentamicin at 30 min post infection. Growth of bacteria was measured by serial dilutions at 5 h after infection. For canonical-inflammasome activation LFn-tagged TcdB (5 μg/mL) and PrgJ (2 μg/mL) along with PA protein were added into opti-MEM culture medium. Cells were centrifuged at 700 x g for 10 min at room temperature, and further incubated at 37°C for 5 hr and 4 hr, respectively. For electroporation, BMNs were seeded into 24-well plate at a density of ~2.5×10^6 cells/well and electroporated with TcdB (10 μg/mL) or PrgJ (4 μg/mL) in opti-MEM medium using Amaxa 4D-Nucleofector Y unit (Lonza). To inhibit phagocytosis, cytochalasin D (APExBIO, 10 μ/mL) was added 30 min before stimulation with PrgJ.

***In vitro* NETs assay—**BMNs were seeded into 96-well plates at a density of 2.5×10^5 cells/well. 16 hr primed BMNs were infection with bacteria at a MOI of 30 for 2 or 3 hr as mentioned above. DNase I (20 U/mL) were added 1 hr post infection to dismantle NETs. NETs were detected by cell-impermeable DNAfluorescent dyes (5 μM Sytox green) along with cell-permeable DNA dyes (1 μg/mL Hoechst). Fluorescent images were taken with a x20 objective with a Keyence BZ-X810.

***In vivo* DNase I treatment—**WT and *Casp1*$^{-/-}$ Mice were challenged intraperitoneally (i.p.) with 2×10^3 CFU of *Yptb-ΔyopM* mutant prepared as mentioned above. After 4hr post-infection, mice were initially administrated via i.p. route with 150 U of DNase I to dismantle NETs or PBS as a control. Mice were treated with the same dose of DNase or PBS approximately the same time every day. Mice were sacrificed 4 d after infection, then spleens and livers were harvested to determine bacterial burden by serial dilutions.

Immunoblot analysis—To detect the inflammasome activation, cells were lysed along with the supernatant using 10x lysis buffer (10% NP-40) followed by 5x SDS loading buffer or using 5x SDS loading buffer directly. For secreted IL-1β, supernatant was collected and added by 5x SDS loading buffer. Cells were lysed by adding comparable volume of 1x SDS loading buffer. Electrophoresis was performed to separate proteins in polyacrylamide gels. Proteins were transferred onto NC membranes and blocked with 0.5% casein for 1 hr at room temperature. The blots were incubated with indicated first antibodies overnight at 4°C,

followed by HRP-conjugated secondary antibodies for 1 hr at room temperature. Images were acquired using ChemiDoc MP Imaging System (Bio-Rad).

Lactate dehydrogenase (LDH) assay—Supernatants or cell lysates were collected at indicated time point after post-infection or stimulation. As a positive control to generate the maximum LDH release, lysis solution was added to untreated cells. Culture medium alone was prepared to correct the background absorbance. The absorbance of supernatants at 492 nm was measured using a microplate reader (FLUOstar Omega; BMG labtech). Cytotoxicity was defined as the percentage of the LDH activity released into the supernatant to the maximum LDH activity.

Flow cytometry—Extent of neutrophil apoptosis after priming was evaluated using FITC Annexin V Apoptosis Detection Kit with PI (BioLegend) according to the manufacturer's instructions. Briefly, 16 hr primed BMNs were collected and washed twice with cold cell staining buffer. 1×10^6 cells were resuspended in 100 μL annexin V binding buffer followed by co-staining with FITC-labeled annexin V (5 μL) and PI (10 μL) for 15 min at room temperature. Cell fluorescence was detected by a BD LSRFortessa and analyzed using FlowJo 10.8.1 software.

Cytokine analysis—IL-1β secretion was determined by ELISA (R&D Systems) according to manufacturer's instructions.

QUANTIFICATION AND STATISTICAL ANALYSIS

Statistical analyses were carried out using GraphPad Prism version 9.0 software. Statistical significance was determined by one-way ANOVA, two-way ANOVA, or two-tailed Student's t-test with a statistical threshold of $p \leq 0.05$. Mouse survival curves were estimated by log-rank (Mantel–Cox) test using Bonferroni-corrected. Error bars depict mean ± SEM. p values of ≤ 0.05 were considered significant (*$p \leq 0.05$, **$p \leq 0.01$, ***$p \leq 0.001$, ns: not significant). All statistical details can be found in the figure legends.

Supplementary Material

Refer to Web version on PubMed Central for supplementary material.

ACKNOWLEDGMENTS

We would like to thank Dr. Daniel Voth for valuable scientific discussions regarding the design of this study, Dr. Jimmy Ballard for sharing LFn-TcdB, and Dr. Jae Jin Chae for sharing *Mefv*$^{-/-}$ mice. We also thank UAMS DLAM for mice breeding and care. We acknowledge our funding sources including AI099222 to J.B.B., AI133236, AI139304, and AI136920 to E.A.M., and GM103625 to Y.A. Y.A. would like also to acknowledge an equipment grant from the UAMS Office of the Vice Chancellor for Research and Innovation

REFERENCES

Aachoui Y, Kajiwara Y, Leaf IA, Mao D, Ting JP, Coers J, Aderem A, Buxbaum JD, and Miao EA (2015). Canonical inflammasomes drive IFN-gamma to prime caspase-11 in defense against a cytosol-invasive bacterium. Cell Host Microbe 18, 320–332. 10.1016/j.chom.2015.07.016. [PubMed: 26320999]

Aachoui Y, Leaf IA, Hagar JA, Fontana MF, Campos CG, Zak DE, Tan MH, Cotter PA, Vance RE, Aderem A, and Miao EA (2013a). Caspase-11 protects against bacteria that escape the vacuole. Science 339, 975–978. 10.1126/science.1230751. [PubMed: 23348507]

Aachoui Y, Sagulenko V, Miao EA, and Stacey KJ (2013b). Inflammasome-mediated pyroptotic and apoptotic cell death, and defense against infection. Curr. Opin. Microbiol 16, 319–326. 10.1016/j.mib.2013.04.004. [PubMed: 23707339]

Agarwal S, Loder SJ, Cholok D, Li J, Bian G, Yalavarthi S, Li S, Carson WF, Hwang C, Marini S, et al. (2019). Disruption of neutrophil extracellular traps (NETs) links mechanical strain to post-traumatic inflammation. Front. Immunol 10, 2148. 10.3389/fimmu.2019.02148. [PubMed: 31708911]

Arita K, Hashimoto H, Shimizu T, Nakashima K, Yamada M, and Sato M (2004). Structural basis for Ca(2+)-induced activation of human PAD4. Nat. Struct. Mol. Biol 11, 777–783. 10.1038/nsmb799. [PubMed: 15247907]

Aubert DF, Xu H, Yang J, Shi X, Gao W, Li L, Bisaro F, Chen S, Valvano MA, and Shao F (2016). A Burkholderia type VI effector deamidates Rho GTPases to activate the pyrin inflammasome and trigger inflammation. Cell Host Microbe 19, 664–674. 10.1016/j.chom.2016.04.004. [PubMed: 27133449]

Barth H, Pfeifer G, Hofmann F, Maier E, Benz R, and Aktories K (2001). Low pH-induced formation of ion channels by clostridium difficile toxin B in target cells. J. Biol. Chem 276, 10670–10676. 10.1074/jbc.M009445200. [PubMed: 11152463]

Bergsbaken T, and Cookson BT (2007). Macrophage activation redirects yersinia-infected host cell death from apoptosis to caspase-1-dependent pyroptosis. PLoS Pathog. 3, e161. 10.1371/journal.ppat.0030161. [PubMed: 17983266]

Brodsky IE, Palm NW, Sadanand S, Ryndak MB, Sutterwala FS, Flavell RA, Bliska JB, and Medzhitov R (2010). A Yersinia effector protein promotes virulence by preventing inflammasome recognition of the type III secretion system. Cell Host Microbe 7, 376–387. 10.1016/j.chom.2010.04.009. [PubMed: 20478539]

Chae JJ, Cho YH, Lee GS, Cheng J, Liu PP, Feigenbaum L, Katz SI, and Kastner DL (2011). Gain-of-function Pyrin mutations induce NLRP3 protein-independent interleukin-1beta activation and severe autoinflammation in mice. Immunity 34, 755–768. 10.1016/j.immuni.2011.02.020. [PubMed: 21600797]

Chen KW, Demarco B, Ramos S, Heilig R, Goris M, Grayczyk JP, Assenmacher CA, Radaelli E, Joannas LD, Henao-Mejia J, et al. (2021). RIPK1 activates distinct gasdermins in macrophages and neutrophils upon pathogen blockade of innate immune signaling. Proc. Natl. Acad. Sci. USA 118, e2101189118. 10.1073/pnas.2101189118. [PubMed: 34260403]

Chen KW, Groβ CJ, Sotomayor FV, Stacey KJ, Tschopp J, Sweet MJ, and Schroder K (2014). The neutrophil NLRC4 inflammasome selectively promotes IL-1beta maturation without pyroptosis during acute Salmonella challenge. Cell Rep. 8, 570–582. 10.1016/j.celrep.2014.06.028. [PubMed: 25043180]

Chen KW, Monteleone M, Boucher D, Sollberger G, Ramnath D, Condon ND, von Pein JB, Broz P, Sweet MJ, and Schroder K (2018). Non-canonical inflammasome signaling elicits gasdermin D-dependent neutrophil extracellular traps. Sci. Immunol 3, eaar6676. 10.1126/sciimmunol.aar6676. [PubMed: 30143554]

Chung LK, and Bliska JB (2016). Yersinia versus host immunity: how a pathogen evades or triggers a protective response. Curr. Opin. Microbiol 29, 56–62. 10.1016/j.mib.2015.11.001. [PubMed: 26638030]

Chung LK, Park YH, Zheng Y, Brodsky IE, Hearing P, Kastner DL, Chae JJ, and Bliska JB (2016). The Yersinia virulence factor YopM hijacks host kinases to inhibit type III effector-triggered activation of the pyrin inflammasome. Cell Host Microbe 20, 296–306. 10.1016/j.chom.2016.07.018. [PubMed: 27569559]

Cunha LD, and Zamboni DS (2013). Subversion of inflammasome activation and pyroptosis by pathogenic bacteria. Front. Cell. Infect. Microbiol 3, 76. 10.3389/fcimb.2013.00076. [PubMed: 24324933]

Fischer FA, Chen KW, and Bezbradica JS (2021). Posttranslational and therapeutic control of gasdermin-mediated pyroptosis and inflammation. Front. Immunol 12, 661162. 10.3389/fimmu.2021.661162. [PubMed: 33868312]

Jorgensen I, Zhang Y, Krantz BA, and Miao EA (2016). Pyroptosis triggers pore-induced intracellular traps (PITs) that capture bacteria and lead to their clearance by efferocytosis. J. Exp. Med 213, 2113–2128. 10.1084/jem.20151613. [PubMed: 27573815]

Just I, Selzer J, Wilm M, von Eichel-Streiber C, Mann M, and Aktories K (1995). Glucosylation of Rho proteins by Clostridium difficile toxin B. Nature 375, 500–503. 10.1038/375500a0. [PubMed: 7777059]

Karmakar M, Minns M, Greenberg EN, Diaz-Aponte J, Pestonjamasp K, Johnson JL, Rathkey JK, Abbott DW, Wang K, Shao F, et al. (2020). N-GSDMD trafficking to neutrophil organelles facilitates IL-1beta release independently of plasma membrane pores and pyroptosis. Nat. Commun 11, 2212. 10.1038/s41467-020-16043-9. [PubMed: 32371889]

Kayagaki N, Warming S, Lamkanfi M, Vande Walle L, Louie S, Dong J, Newton K, Qu Y, Liu J, Heldens S, et al. (2011). Non-canonical inflammasome activation targets caspase-11. Nature 479,117–121. 10.1038/nature10558. [PubMed: 22002608]

Kearney PL, Bhatia M, Jones NG, Yuan L, Glascock MC, Catchings KL, Yamada M, and Thompson PR (2005). Kinetic characterization of protein arginine deiminase 4: a transcriptional corepressor implicated in the onset and progression of rheumatoid arthritis. Biochemistry 44, 10570–10582. 10.1021/bi050292m. [PubMed: 16060666]

Kovacs SB, Oh C, Maltez VI, McGlaughon BD, Verma A, Miao EA, and Aachoui Y (2020). Neutrophil caspase-11 is essential to defend against a cytosol-invasive bacterium. Cell Rep. 32, 107967. 10.1016/j.celrep.2020.107967. [PubMed: 32726630]

Kuida K, Lippke JA, Ku G, Harding MW, Livingston DJ, Su MS, and Flavell RA (1995). Altered cytokine export and apoptosis in mice deficient in interleukin-1 beta converting enzyme. Science 267, 2000–2003. 10.1126/science.7535475. [PubMed: 7535475]

LaRock CN, and Cookson BT (2012). The Yersinia virulence effector YopM binds caspase-1 to arrest inflammasome assembly and processing. Cell Host Microbe 12, 799–805. 10.1016/j.chom.2012.10.020. [PubMed: 23245324]

Maltez VI, Tubbs AL, Cook KD, Aachoui Y, Falcone EL, Holland SM, Whitmire JK, and Miao EA (2015). Inflammasomes coordinate pyroptosis and natural killer cell cytotoxicity to clear infection by a ubiquitous environmental bacterium. Immunity 43, 987–997. 10.1016/j.immuni.2015.10.010. [PubMed: 26572063]

Marketon MM, DePaolo RW, DeBord KL, Jabri B, and Schneewind O (2005). Plague bacteria target immune cells during infection. Science 309, 1739–1741. 10.1126/science.1114580. [PubMed: 16051750]

McPhee JB, Mena P, and Bliska JB (2010). Delineation of regions of the Yersinia YopM protein required for interaction with the RSK1 and PRK2 host kinases and their requirement for interleukin-10 production and virulence. Infect. Immun 78, 3529–3539. 10.1128/IAI.00269-10. [PubMed: 20515922]

Miao EA, Leaf IA, Treuting PM, Mao DP, Dors M, Sarkar A, Warren SE, Wewers MD, and Aderem A (2010). Caspase-1-induced pyroptosis is an innate immune effector mechanism against intracellular bacteria. Nat. Immunol 11, 1136–1142. 10.1038/ni.1960. [PubMed: 21057511]

Miralda I, Uriarte SM, and McLeish KR (2017). Multiple Phenotypic Changes Define Neutrophil Priming. Frontiers in cellular and infection microbiology 7, 217. 10.3389/fcimb.2017.00217. [PubMed: 28611952]

Monack DM, Mecsas J, Ghori N, and Falkow S (1997). Yersinia signals macrophages to undergo apoptosis and YopJ is necessary for this cell death. Proc. Natl. Acad. Sci. USA 94, 10385–10390. 10.1073/pnas.94.19.10385. [PubMed: 9294220]

Oh C, Verma A, Hafeez M, Hogland B, and Aachoui Y (2021). Shigella OspC3 suppresses murine cytosolic LPS sensing. iScience 24, 102910. 10.1016/j.isci.2021.102910. [PubMed: 34409271]

Papayannopoulos V, Metzler KD, Hakkim A, and Zychlinsky A (2010). Neutrophil elastase and myeloperoxidase regulate the formation of neutrophil extracellular traps. J. Cell Biol 191, 677–691. 10.1083/jcb.201006052. [PubMed: 20974816]

Paquette N, Conlon J, Sweet C, Rus F, Wilson L, Pereira A, Rosadini CV, Goutagny N, Weber ANR, Lane WS, et al. (2012). Serine/threonine acetylation of TGFbeta-activated kinase (TAK1) by Yersinia pestis YopJ inhibits innate immune signaling. Proc. Natl. Acad. Sci. USA 109, 12710–12715. 10.1073/pnas.1008203109. [PubMed: 22802624]

Peterson LW, Philip NH, DeLaney A, Wynosky-Dolfi MA, Asklof K, Gray F, Choa R, Bjanes E, Buza EL, Hu B, et al. (2017). RIPK1-dependent apoptosis bypasses pathogen blockade of innate signaling to promote immune defense. J. Exp. Med 214, 3171–3182. 10.1084/jem.20170347. [PubMed: 28855241]

Philip NH, Dillon CP, Snyder AG, Fitzgerald P, Wynosky-Dolfi MA, Zwack EE, Hu B, Fitzgerald L, Mauldin EA, Copenhaver AM, et al. (2014). Caspase-8 mediates caspase-1 processing and innate immune defense in response to bacterial blockade of NF-kappaB and MAPK signaling. Proc. Natl. Acad. Sci. USA 111, 7385–7390. 10.1073/pnas.1403252111. [PubMed: 24799700]

Qa'Dan M, Spyres LM, and Ballard JD (2000). pH-induced conformational changes in Clostridium difficile toxin B. Infect. Immun 68, 2470–2474. 10.1128/IAI.68.5.2470-2474.2000. [PubMed: 10768933]

Ratner D, Orning MPA, Proulx MK, Wang D, Gavrilin MA, Wewers MD, Alnemri ES, Johnson PF, Lee B, Mecsas J, et al. (2016). The Yersinia pestis effector YopM inhibits pyrin inflammasome activation. PLoS Pathog. 12, e1006035. 10.1371/journal.ppat.1006035. [PubMed: 27911947]

Ryu JC, Kim MJ, Kwon Y, Oh JH, Yoon SS, Shin SJ, Yoon JH, and Ryu JH (2017). Neutrophil pyroptosis mediates pathology of P. aeruginosa lung infection in the absence of the NADPH oxidase NOX2. Mucosal Immunol. 10, 757–774. 10.1038/mi.2016.73. [PubMed: 27554297]

Sarhan J, Liu BC, Muendlein HI, Li P, Nilson R, Tang AY, Rongvaux A, Bunnell SC, Shao F, Green DR, and Poltorak A (2018). Caspase-8 induces cleavage of gasdermin D to elicit pyroptosis during Yersinia infection. Proc. Natl. Acad. Sci. USA 115, E10888–E10897. 10.1073/pnas.1809548115. [PubMed: 30381458]

Schoberle TJ, Chung LK, McPhee JB, Bogin B, and Bliska JB (2016). Uncovering an important role for YopJ in the inhibition of caspase-1 in activated macrophages and promoting Yersinia pseudotuberculosis virulence. Infect. Immun 84, 1062–1072. 10.1128/IAI.00843-15. [PubMed: 26810037]

Shannon JG, Hasenkrug AM, Dorward DW, Nair V, Carmody AB, and Hinnebusch BJ (2013). Yersinia pestis subverts the dermal neutrophil response in a mouse model of bubonic plague. mBio 4, e00170–e00113. 10.1128/mBio.00170-13. [PubMed: 23982068]

Shi J, Zhao Y, Wang K, Shi X, Wang Y, Huang H, Zhuang Y, Cai T, Wang F, and Shao F (2015). Cleavage of GSDMD by inflammatory caspases determines pyroptotic cell death. Nature 526, 660–665. 10.1038/nature15514. [PubMed: 26375003]

Simonet M, and Falkow S (1992). Invasin expression in Yersinia pseudotuberculosis. Infect. Immun 60, 4414–4417. 10.1128/iai.60.10.4414-4417.1992. [PubMed: 1398952]

Sollberger G, Choidas A, Burn GL, Habenberger P, Di Lucrezia R, Kordes S, Menninger S, Eickhoff J, Nussbaumer P, Klebl B, et al. (2018). Gasdermin D plays a vital role in the generation of neutrophil extracellular traps. Sci. Immunol 3, eaar6689. 10.1126/sciimmunol.aar6689. [PubMed: 30143555]

Son S, Yoon SH, Chae BJ, Hwang I, Shim DW, Choe YH, Hyun YM, and Yu JW (2021). Neutrophils facilitate prolonged inflammasome response in the DAMP-Rich inflammatory milieu. Front. Immunol 12, 746032. 10.3389/fimmu.2021.746032. [PubMed: 34659244]

Spyres LM, Qa'Dan M, Meader A, Tomasek JJ, Howard EW, and Ballard JD (2001). Cytosolic delivery and characterization of the TcdB glucosylating domain by using a heterologous protein fusion. Infect. Immun 69, 599–601. 10.1128/IAI.69.1.599-601.2001. [PubMed: 11119561]

Sutterwala FS, Mijares LA, Li L, Ogura Y, Kazmierczak BI, and Flavell RA (2007). Immune recognition of Pseudomonas aeruginosa mediated by the IPAF/NLRC4 inflammasome. J. Exp. Med 204,3235–3245. 10.1084/jem.20071239. [PubMed: 18070936]

Thiam HR, Wong SL, Qiu R, Kittisopikul M, Vahabikashi A, Goldman AE, Goldman RD, Wagner DD, and Waterman CM (2020). NETosis proceeds by cytoskeleton and endomembrane disassembly and PAD4-mediated chromatin decondensation and nuclear envelope rupture. Proc. Natl. Acad. Sci. USA 117, 7326–7337. 10.1073/pnas.1909546117. [PubMed: 32170015]

Vareechon C, Zmina SE, Karmakar M, Pearlman E, and Rietsch A (2017). Pseudomonas aeruginosa effector ExoS inhibits ROS production in human neutrophils. Cell Host Microbe 21, 611–618.e5. 10.1016/j.chom.2017.04.001. [PubMed: 28494242]

Viboud GI, and Bliska JB (2005). Yersinia outer proteins: role in modulation of host cell signaling responses and pathogenesis. Annu. Rev. Microbiol 59, 69–89. 10.1146/annurev.micro.59.030804.121320. [PubMed: 15847602]

Wang Y, Li M, Stadler S, Correll S, Li P, Wang D, Hayama R, Leonelli L, Han H, Grigoryev SA, et al. (2009). Histone hypercitrullination mediates chromatin decondensation and neutrophil extracellular trap formation. J. Cell Biol 184,205–213. 10.1083/jcb.200806072. [PubMed: 19153223]

Xu H, Yang J, Gao W, Li L, Li P, Zhang L, Gong YN, Peng X, Xi JJ, Chen S, et al. (2014). Innate immune sensing of bacterial modifications of Rho GTPases by the Pyrin inflammasome. Nature 513,237–241.10.1038/nature13449. [PubMed: 24919149]

Zhao Y, Yang J, Shi J, Gong YN, Lu Q, Xu H, Liu L, and Shao F (2011). The NLRC4 inflammasome receptors for bacterial flagellin and type III secretion apparatus. Nature 477, 596–600. 10.1038/nature10510. [PubMed: 21918512]

Highlights

- Extracellular *Yptb-ΔyopM* drives caspase-1-GSDMD pyroptosis in neutrophils
- Neutrophil inflammasomes discriminate plasma membrane from endosome membrane signals
- Caspase-1-GSDMD pyroptosis induces PAD4-dependent H3 citrullination and NET extrusion
- Pyroptosis-dependent NETs are critical to protect hosts against *Yptb-ΔyopM* infection

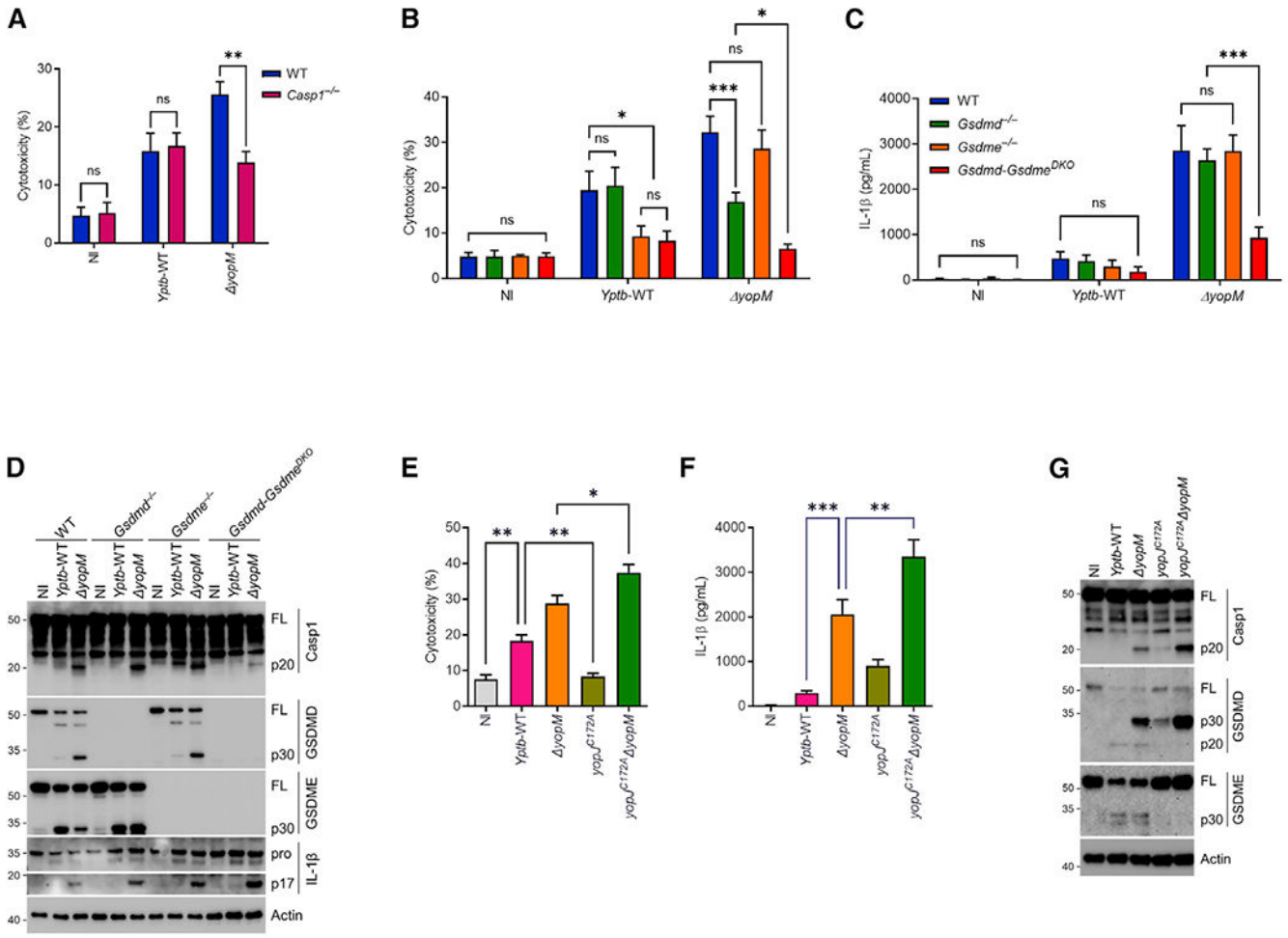

Figure 1. Neutrophil detection of *Y. pseudotuberculosis* Δ*yopM* promotes two distinct signaling pathways to drive GSDMD- and GSDME-dependent pyroptosis

(A–D) Indicated BMNs were primed for 3 h and subsequently infected with *Yptb*-WT or *ΔyopM* at MOI 30 for 3 h. Cytotoxicity was determined by LDH release assay (A and B), IL-1β release was determined by ELISA (C), and immunoblots were probed with the indicated antibodies (D).

(E–G) WT BMNs were primed (3 h), followed by infection with *Yptb*-WT, *ΔyopM* *yopJ*^{C172A}, or *yopJ*^{C172A}*ΔyopM* at MOI 30. LDH release (E), IL-1β release (F), and inflammasome activation (G) were monitored.

Actin was used as a loading control. Data are mean ± SEM of three independent experiments. Statistical significance was analyzed by two-way ANOVA followed by Bonferroni's multiple comparison test (A– C) or by one-way ANOVA followed by Tukey's multiple comparison test (E and F). *p ≤ 0.05, **p ≤ 0.01, ***p ≤ 0.001, ns, not significant. NI, non-infected.

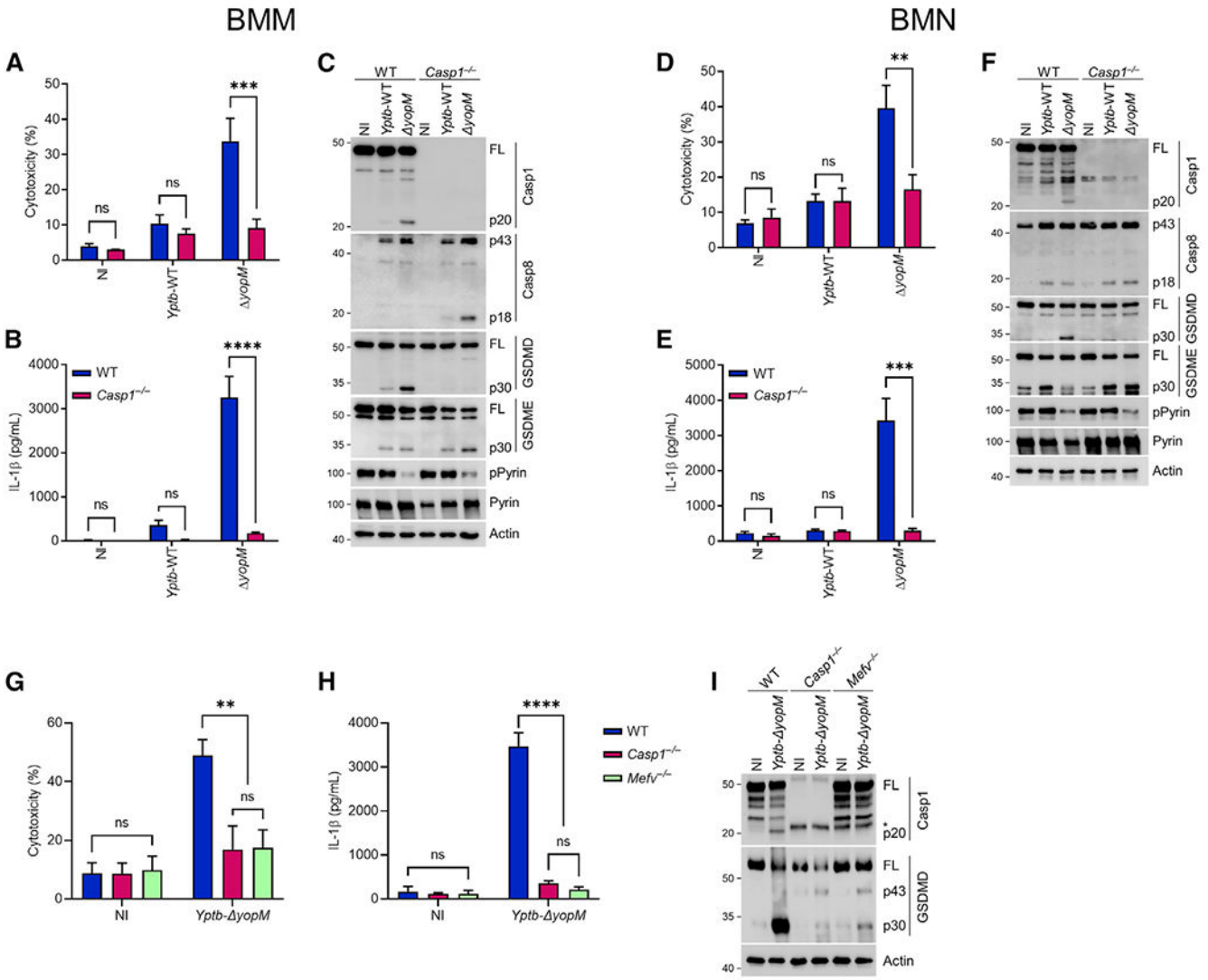

Figure 2. Pyrin drives neutrophil caspase-1-dependent pyroptosis in response to *Y. pseudotuberculosis* Δ*yopM* infection

Indicated BMMs (A–C) and BMNs (D–I) were primed for 16 h, then left non-infected (NI) or infected with either *Yptb*-WT or *ΔyopM* at MOI 30 for 3 h. Cytotoxicity was determined by LDH release assay (A, D, and G), IL-1β release was determined by ELISA (B, E, and H), and immunoblots were probed with the indicated antibodies (C, F, and I). Actin was used as a loading control. Data are mean ± SEM of three independent experiments. Cytotoxicity and IL-1β levels were analyzed by two-way ANOVA followed by Bonferroni's multiple comparison test (A, B, D, E, G, and H). **p ≤ 0.01, ***p ≤ 0.001, ****p ≤ 0.0001, ns, not significant. Asterisk indicates a non-specific band (I).

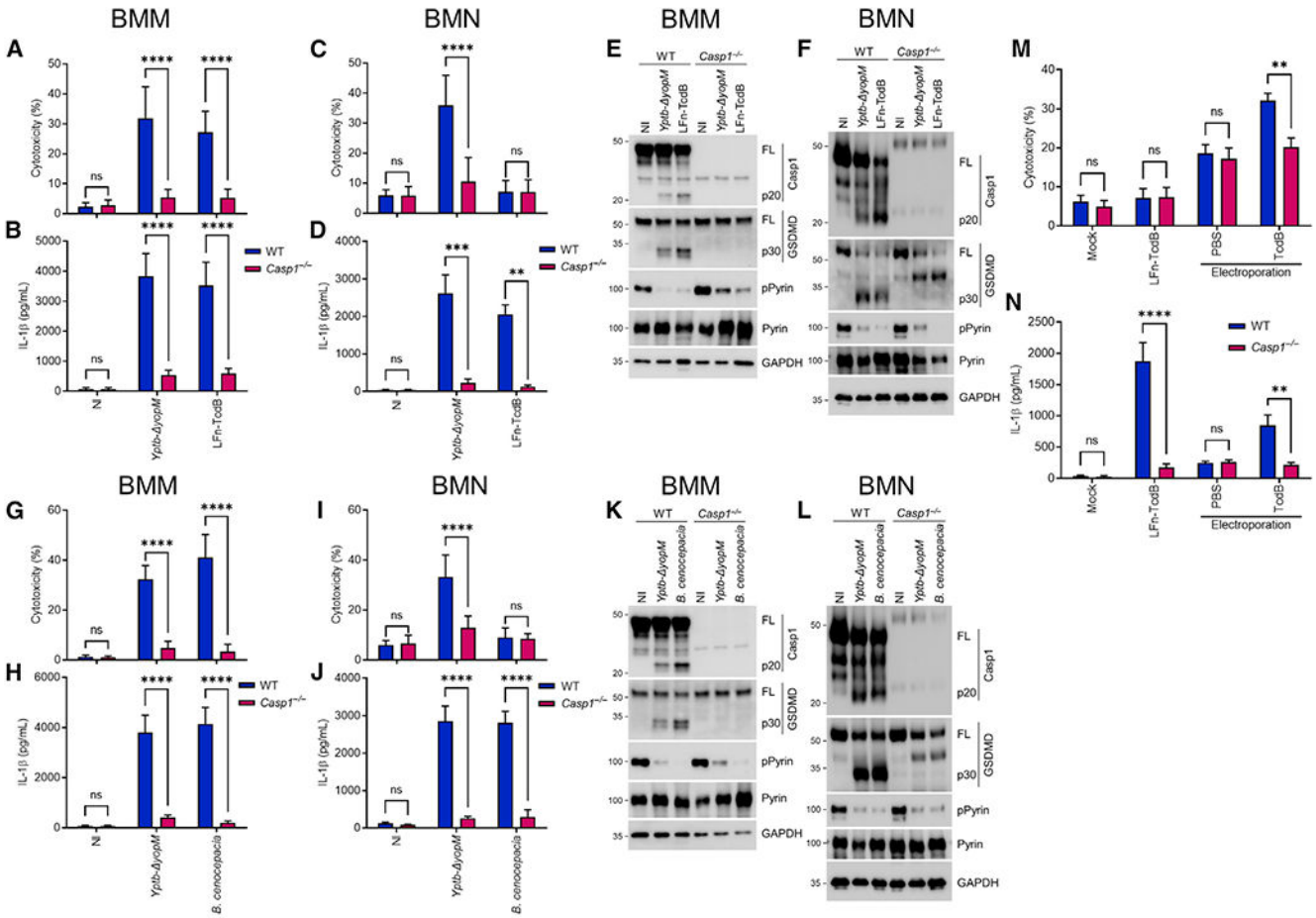

Figure 3. Neutrophil pyrin inflammasome discriminates between agonists that access the cytosol from plasma membrane or endocytic route to promote pyroptosis

(A–F) Primed (16 h) WT and *Casp1*$^{-/-}$ BMMs (A, B, and E) and BMNs (C, D, and F) were either infected with *Yptb-ΔyopM* (30 MOI) for 3 h or stimulated with LFn-TcdB (5 μg/mL) for 5 h.

(G–L) Primed (16 h) WT and *Casp1*$^{-/-}$ BMMs (G, H, and K) and BMNs (I, J, and L) were either infected with *Yptb-ΔyopM* (30 MOI) or *B. cenocepacia* (30 MOI) for 3 h.

(M and N) WT and *Casp1*$^{-/-}$ BMNs were primed (3 h) and either stimulated with LFn-TcdB (5 μg/mL) or electroporated with TcdB (10 μg/mL) for 5 h.

Cytotoxicity was determined by LDH release assay (A, C, G, I, and N), IL-1β release was determined by ELISA (B, D, H, J, and M), and immunoblots were probed with the indicated antibodies (E, F, K, and L). Actin was used as a loading control. Data are mean ± SEM of three independent experiments. Cytotoxicity and IL-1β levels were analyzed by two-way ANOVA followed by Bonferroni's multiple comparison test (A–D, G–J, M, and N). **p ≤ 0.01, ***p ≤ 0.001, ****p ≤ 0.0001, ns, not significant

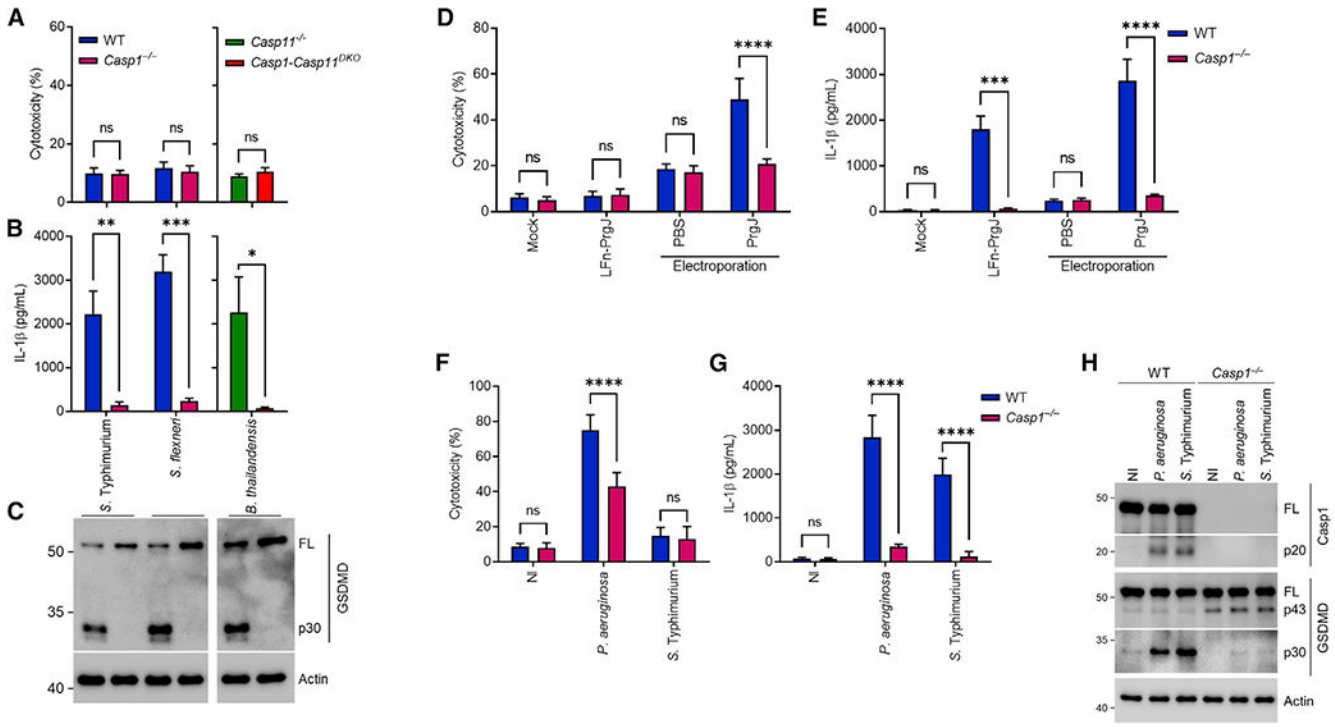

Figure 4. Neutrophil NLRC4 inflammasomes respond to plasma-membrane-dependent T3SS injection by driving caspase-1 pyroptosis

(A–C) Indicated BMNs were primed (16 h) and then infected with *S. typhimurium, S. flexneri*, or *B. thailandensis* at MOI 30 for 3 h.

(D and E) WT and *Casp1*$^{-/-}$ BMNs were primed (3 h) and either stimulated with LFn-PrgJ (2 μg/mL) for 4 h or electroporated with PrgJ (4 μg/mL) for 2 h.

(F–H) Primed (16 h) WT and *Casp1*$^{-/-}$ BMNs were infected with *P. aeruginosa* or *S. typhimurium* at MOI 30 for 3 h.

Cytotoxicity was determined by LDH release assay (A, D, and F), IL-1β release was determined by ELISA (B, E, and G), and immunoblots were probed with the indicated antibodies (C and H). Actin was used as a loading control. Bar represents mean ± SEM. Data are representative of three independent experiments. Cytotoxicity and IL-1β levels were analyzed by two-way ANOVA followed by Bonferroni's multiple comparison test (A, B, and D–G). *$p \leq 0.05$, **$p \leq 0.01$, ***$p \leq 0.001$, ****$p \leq 0.0001$, ns, not significant.

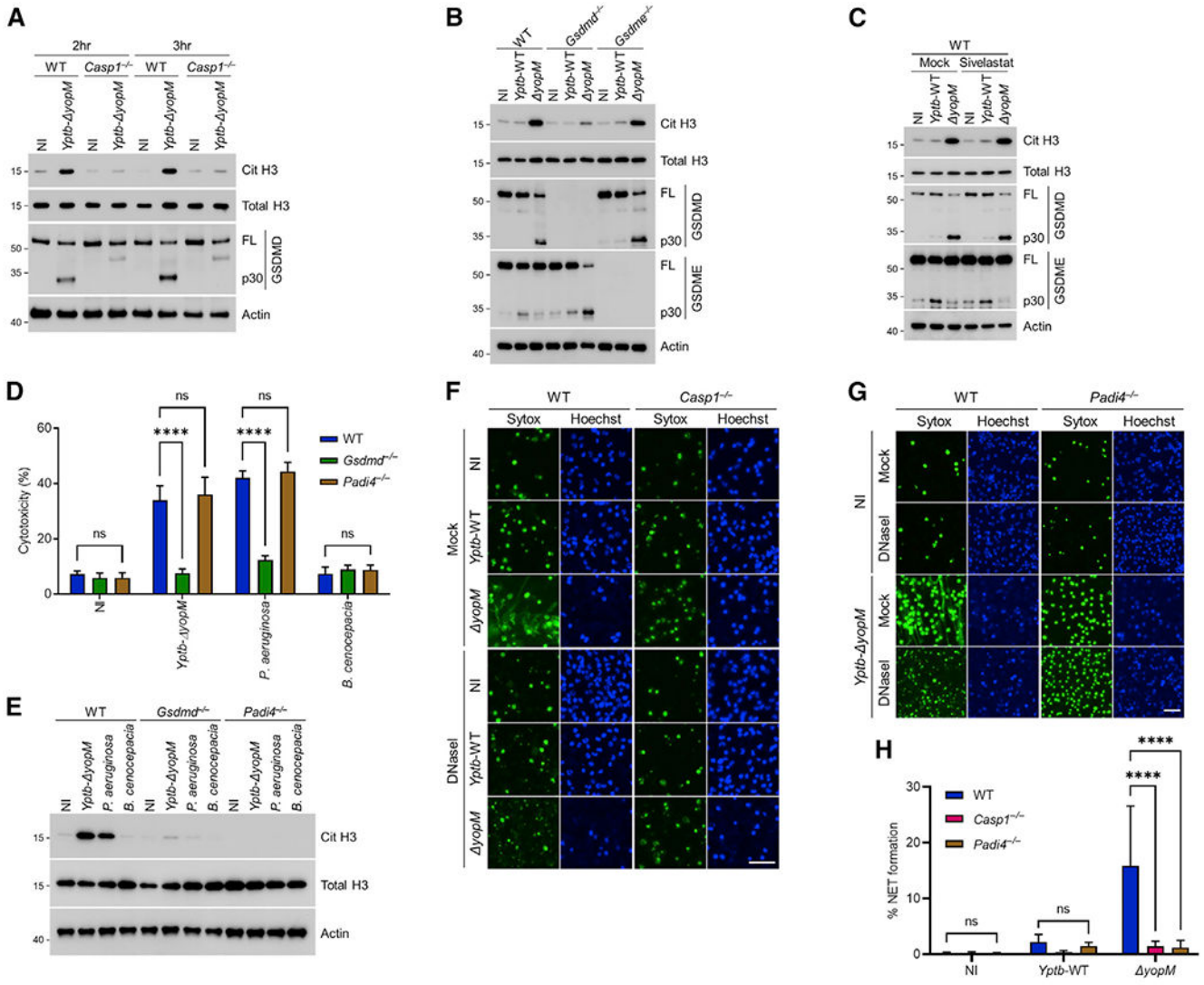

Figure 5. Caspase-1-GSDMD-driven pyroptosis promotes PAD4-dependent histone H3 citrullination and NET extrusion

(A) WT and *Casp1*$^{-/-}$ BMNs were primed for 16 h and then infected with *Yptb-ΔyopM* at MOI 30 for indicated time points (2 or 3 h).

(B) Indicated BMNs were primed for 16 h and then infected with *Yptb*-WT or *ΔyopM* at MOI 30 for 2 h.

(C) Primed (16 h) WT BMNs were treated or not with NE inhibitor sivelestat (1 μg/mL) and infected with either *Yptb*-WT or *ΔyopM* at MOI 30 for 2 h.

(D and E) Indicated BMNs were primed (16 h) and then infected with *Yptb-ΔyopM*, *P. aeruginosa*, or *B. cenocepacia* at MOI 30 for 2 h.

(F–H) Indicated BMNs were primed for 16 h and then infected with *Yptb*-WT or *ΔyopM* at MOI 30 with or without DNase I for 2 h. BMNs were stained with Hoechst and Sytox green to detect NET formation. Microscopy images were quantified for NETs, where cells with spread DNA were counted as cells undergoing NET extrusion. Total Hoechst+ cells counted

in excessively exposed images to determine the denominator in the percent NET formation (H).

Cytotoxicity was determined by LDH release assay (D), and immunoblots were probed with the indicated antibodies (A–C and E). Actin was used as a loading control. Data are mean ± SEM of three independent experiments. Scale bar, 40 μm (F and G). Cytotoxicity and percentage of NET formation were analyzed by two-way ANOVA followed by Bonferroni's multiple comparison test (D and H). ****$p \leq 0.0001$, ns, not significant.

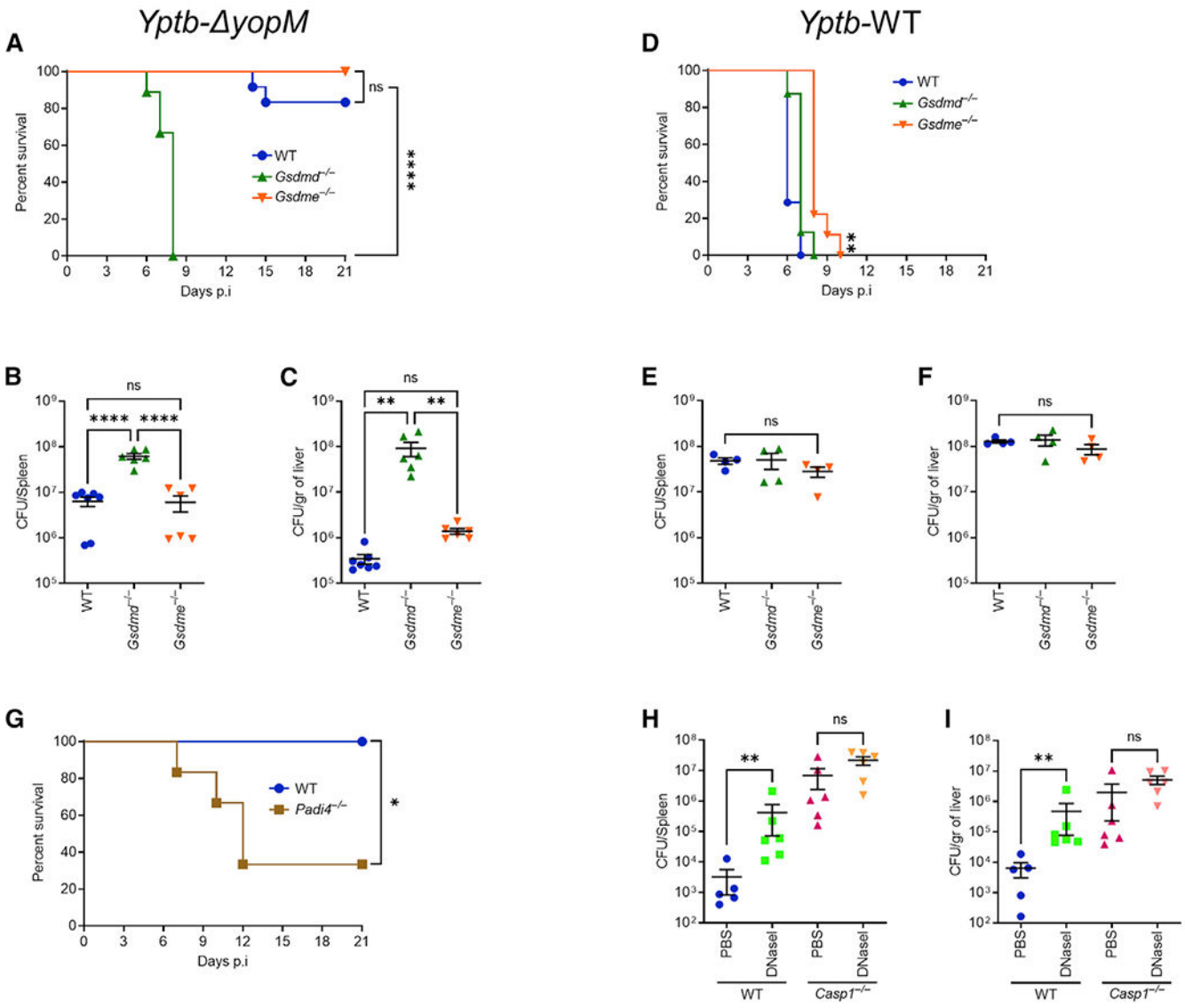

Figure 6. Neutrophil pyrin-driven GSDMD pyroptosis and PAD4 are critical in defense against *Y. pseudotuberculosis* ΔyopM, whereas GSDME is deleterious

(A–G) Indicated mice were infected intranveously (i.v.) with 2×10^3 colony-forming units (CFUs) of *Yptb-ΔyopM* (A–C and G) or *Yptb*-WT (D–F). Survival was monitored twice daily for 21 days (A, D, and G), and bacterial loads in spleen (B and E) and liver (C and F) were determined 5 days post-infection. Dead mouse (*Il1b-Il18*^{DKO}, n = 1, indicated as "†"in the graph) was excluded from statistical analysis.

(H and I) WT and *Casp1*$^{-/-}$ mice were infected i.p. with 2×10^3 CFUs of *Yptb-ΔyopM*. Then, mice were treated daily by 150 U of DNase I or PBS. Bacterial loads in spleen (H) and liver (I) were determined 4 days post-infection.

Data are pooled from at least two independent experiments. Bar represents mean ± SEM. Survival curves were compared using log rank (Mantel-Cox) test with Bonferroni-corrected test (A, D, and G). For bacterial loads, statistical significance was determined using one-way ANOVA followed by Tukey's multiple comparison test (B, C, E, and F) or two-way ANOVA

followed by Bonferroni's multiple comparison test (H and I). *p ≤ 0.05, **p ≤ 0.01, ****p ≤ 0.0001, ns, not significant.

KEY RESOURCES TABLE

REAGENT or RESOURCE	SOURCE	IDENTIFIER
Antibodies		
Rabbit anti-mouse GSDMD (clone EPR19828)	Abcam	Cat# ab209845; RRID: AB_2783550
Rabbit anti-DFNA5/GSDME (clone EPR19859)	Abcam	Cat# ab215191; RRID: AB_2737000
Mouse anti-mouse caspase-1 p20 (clone Casper-1)	AdipoGen	Cat# AG-20B-0042-C100; RRID: AB_2755041
Rabbit anti-cleaved Caspase-7 (Asp198) (clone D6H1)	Cell Signaling Technology	Cat# 8438; RRID: AB_11178377
Rabbit anti-cleaved Caspase-8 (clone D5B2)	Cell Signaling Technology	Cat# 8592; RRID: AB_10891784
Rabbit anti-Ipaf (NLRC4)	Millipore	Cat# 06-1125; RRID: AB_10807029
Rabbit anti-Asc pAb (AL177)	AdipoGen	Cat# AG-25B-0006; RRID: AB_2490440
Goat anti-Mouse IL-1 beta/IL-1F2	R&D Systems	Cat# AF-401-NA; RRID:AB_416684
Rabbit anti-Pyrin(phospho S205) (clone EPR19567)	Abcam	Cat# ab201784
Rabbit anti-Pyrin (clone EPR18676)	Abcam	Cat# ab195975
Rabbit anti-Histone H3 (clone 96C10)	Cell Signaling Technology	Cat# 3638; RRID: AB_1642229
Rabbit anti-Histone H3 (citrulline R2 + R8 + R17)	Abcam	Cat# ab5103; RRID: AB_304752
Mouse anti-actin (clone ACTN05 (C4))	Thermo Fisher Scientific	Cat# MA5-11869; RRID: AB_11004139
Rabbit anti-GAPDH (Clone 14C10)	Cell Signaling Technology	Cat# 2118; PRID: AB_561053
Bacterial and virus strains		
Y. pseudotuberculosis (32777) wild-type	Simonet and Falkow, 1992	N/A
Y. pseudotuberculosis ΔyopM	McPhee et al., 2010	N/A
Y. pseudotuberculosis yopJ^{C172A}	Schoberle et al., 2016	N/A
Y. pseudotuberculosis yopJ^{C172A}*ΔyopM*	Schoberle et al., 2016	N/A
P. aeruginosa (PAO1) wild-type	Colin Manoil (University of Washington)	N/A
P. aeruginosa (PAO1) *ΔexoS*	Colin Manoil (University of Washington)	N/A
P. aeruginosa (PAK) wild-type	Bob Ernst (University of Maryland)	N/A
S. Typhimurium (CS401)	Samuel I Miller (University of Washington)	N/A
B. cenocepacia (CGD isolate)	Maltez et al., 2015	N/A
B. thailandensis (E264-1, passaged through *Casp1-Casp11^{DKO}mice*)	Aachoui et al., 2015	N/A
Biological samples		
Ultrapure LPS, *E. coli* O111:B4	InvivoGen	Cat# tlrl-3pelps
Chemicals, peptides, and recombinant proteins		
Recombinant mouse IFN-γ	PeproT ech	Cat# 315-05
Deoxyribonuclease I	Promega	Cat# M6101
Sivelestat sodium salt	Tocris	Cat# 3535
Cytochalasin D	APExBIO	Cat# B6645

REAGENT or RESOURCE	SOURCE	IDENTIFIER
SYTOX green	Thermo Fisher Scientific	Cat# S7020
Hoechst 33342	Thermo Fisher Scientific	Cat# H3570
Hoechst 33342	BD Bioscience	Cat# 561908
LFn-PrgJ	Zhao et al., 2011	N/A
LFn-TcdB	Spyres et al., 2001	N/A
Critical commercial assays		
Mouse IL-1 beta/IL-1F2 DuoSet ELISA	R&D Systems	Cat# DY401
Neutrophil Isolation Kit, mouse	Miltenyi Biotec	Cat# 130-097-658
AD2 4D-NucleofectorTM Y Kit	Lonza	Cat# V4YP-2A24
FITC Annexin V Apoptosis Detection Kit with PI	Biolegend	Cat# 640914
Experimental models: Organisms/strains		
Mouse: Wild type (WT): C57BL/6J	The Jackson Laboratory	JAX# 000664
Mouse: *Nlrc4-Asc*^{DKO}: C57BL/6N	Aachoui et al., 2015	N/A
Mouse: *Casp1*$^{-/-}$: C57BL/6N	The Jackson Laboratory	JAX# 032662
Mouse: *Casp11*$^{-/-}$: C57BL/6N	Kayagaki et al., 2011	N/A
Mouse: *Casp1*$^{-/-}$ *Casp11*$^{129mut/129mut}$ referred to as *Casp1-Casp11*^{DKO}	Kuida et al., 1995	N/A
Mouse: *Gsdmd*$^{-/-}$: C57BL/6	The Jackson Laboratory	JAX# 032663
Mouse: *Gsdme*$^{-/-}$: C57BL/6	The Jackson Laboratory	JAX# 032411
Mouse: *Mefv*$^{-/-}$: C57BL/6	Chae et al., 2011	N/A
Mouse: *Padi4*$^{-/-}$: C57BL/6J	The Jackson Laboratory	JAX# 030315
Software and algorithms		
Prism 9.0	GraphPad	https://www.graphpad.com
FlowJo 10.8.1	BD Biosciences	https://www.flowjo.com